European Journal of Neuroscience, Vol. 20, pp. 3244–3258, 2004

Gene expression profiling of the rat superior olivary complex using serial analysis of gene expression

Alexander Koehl,[1] Nicole Schmidt,[1] Anne Rieger,[1] Sara M. Pilgram,[2] Ivica Letunic,[3] Peer Bork,[3] Florentina Soto,[2] Eckhard Friauf[1] and Hans Gerd Nothwang[1]
[1]Abteilung Tierphysiologie, Technische Universität Kaiserslautern, Postfach 3049, 67653 Kaiserslautern, Germany
[2]Abteilung Molekulare Biologie neuronaler Signale, Max-Planck-Institut für Experimentelle Medizin, Göttingen, Germany
[3]EMBL, Heidelberg, Germany

Keywords: energy metabolism, gene expression, purinergic receptor, SAGE, Sprague–Dawley rats

Abstract

The superior olivary complex (SOC) is an auditory brainstem region that represents a favourable system to study rapid neurotransmission and the maturation of neuronal circuits. Here we performed serial analysis of gene expression (SAGE) on the SOC in 60-day-old Sprague–Dawley rats to identify genes specifically important for its function and to create a transcriptome reference for the subsequent identification of age-related or disease-related changes. Sequencing of 31 035 tags identified 10 473 different transcripts. Fifty-seven per cent of the unique tags with a count greater than four were statistically more highly represented in the SOC than in the hippocampus. Among them were genes encoding proteins involved in energy supply, the glutamate/glutamine shuttle, and myelination. Approximately 80 plasma membrane transporters, receptors, channels, and vesicular transporters were identified, and 25% of them displayed a significantly higher expression level in the SOC than in the hippocampus. Some of the plasma membrane proteins were not previously characterized in the SOC, e.g. the purinergic receptor subunit $P2X_6$ and the metabotropic GABA receptor Gpr51. Differential gene expression between SOC and hippocampus was confirmed using RNA *in situ* hybridization or immunohistochemistry. The extensive gene inventory presented here will alleviate the dissection of the molecular mechanisms underlying specific SOC functions and the comparison with other SAGE libraries from brain will ease the identification of promoters to generate region-specific transgenic animals. The analysis will be part of the publicly available database ID-GRAB.

Introduction

To a large extent, the pattern of expressed genes (i.e. the transcriptome) determines brain function. Knowledge about the transcriptome is therefore a fundamental requirement for in-depth understanding of neuronal processes. Genomics, through various concerted actions such as the genome projects in man, mouse, and rat, has provided information of almost the full complement of genes in these species (Lander *et al*., 2001; Waterston *et al*., 2002; Gibbs *et al*., 2004). These genomic tools, together with the invention of methods for large-scale gene expression analysis, now allow the identification of gene expression profiles to an unprecedented extent.

One of the recently developed techniques for large-scale mRNA expression profiling is the serial analysis of gene expression (SAGE) (Velculescu *et al*., 1995). SAGE is a sequence-based method that does not require prior knowledge of the expressed genes. It is based on the reduction of each expressed transcript to a short (10–11 base-pair-long), yet representative, sequence (tag) defined by the last (most-3′) occurrence of a certain restriction enzyme recognition site in the cDNA. In theory, ten base-pair-long tags can discriminate $4^{10} = 1048\,576$ sequences. The tags are concatenated into long molecules, and these concatemers yield information on multiple transcripts in a single sequence reaction. This considerably increases the efficacy compared to conventional expressed sequence tag (EST) projects. Furthermore, the number of times (counts) a particular tag is detected in a SAGE library provides a quantitative and digital measure of gene expression, which enables easy comparison between different SAGE libraries (Velculescu *et al*., 1995; Ruan *et al*., 2004).

Studies of the mammalian brain transcriptome have to take into account that the brain is composed of a plethora of anatomically and physiologically distinct regions. One of the main challenges in neurobiology is therefore the identification of the specific transcriptomes of these different regions. To this end, we have started an extensive analysis of the mRNA complement of the superior olivary complex (SOC) using SAGE. The SOC is an essential processing centre in the mammalian auditory brainstem. It is the first binaural structure within the auditory pathway, i.e. it receives input from both ears. It consists of several nuclei, the major ones being the lateral superior olive (LSO), the medial superior olive (MSO), and the medial nucleus of the trapezoid body (MNTB). These nuclei are involved in sound localization by computing time or level differences between the two ears (Grothe, 2003). As accurate timing of auditory information is essential for this computation, auditory brainstem neurons display specializations that are not observed in any other sensory circuitry; very fast synaptic transmission and morphologically unusual synapses are striking examples (Oertel, 1999; Trussell, 1999; von Gersdorff & Borst, 2002). The important role in auditory information processing, together with the exquisite specializations, have made the SOC a favourable system to study neurotransmission in great detail (Trussell, 1999; Schneggenburger *et al*., 2002). The SOC is also widely used to study the structure and function of inhibitory neuronal circuits, as well

Correspondence: Dr Hans Gerd Nothwang, as above.
E-mail: nothwang@rhrk.uni-kl.de

Received 9 June 2004, revised 8 September 2004, accepted 1 October 2004

doi:10.1111/j.1460-9568.2004.03791.x

as their formation during development. The projection from the MNTB to the LSO represents an advantageous structure for analysing the maturation of inhibitory synapses, as the pre- and postsynaptic neurons are clearly separated anatomically (Sanes & Friauf, 2000). Studies on this projection led to the detailed description of a refinement of neuronal circuits and to the discovery of a developmental switch from GABA release to glycine release at single synaptic terminals (Kim & Kandler, 2003; Nabekura *et al*., 2004).

Our SAGE analysis yielded more than 10 000 different transcripts in the adult rat SOC. To identify genes specifically important for the function of this auditory centre, we compared the data with those from a SAGE library of the hippocampus (Datson *et al*., 2001). The comparison revealed many genes more highly expressed in the SOC, thus being candidates for SOC-related function. To confirm the differential expression pattern, *in situ* hybridization and immunohistochemistry were performed. As gene expression is highly dynamic and a function of development, ageing, and disease, these validated data will serve as a transcriptome reference for future expression analyses aimed at the identification of developmental or disease-related changes in the SOC.

Materials and methods

Tissue preparation

Sprague–Dawley rats of both genders [at postnatal day (P) 60 for SAGE and immunohistochemistry and at an age of 8–9 weeks for *in situ* hybridization analysis] were deeply anaesthetized by a peritoneal injection of 700 mg/kg chloral hydrate and killed by decapitation. All protocols complied with the current German Animal Protection Law and were approved by the local animal care and use committee (Landesuntersuchungsamt Koblenz, Germany). The brains were rapidly removed and dissected in a chilled (≈4 °C) solution containing (mM): 25 $NaHCO_3$, 2.5 KCl, 1.25 NaH_2PO_4, 1 $MgCl_2$, 2 $CaCl_2$, 260 D-glucose, 2 sodium pyruvate, 3 *myo*-inositol and 1 kynurenic acid, pH 7.4. Coronal slices (300-μm thick) containing the SOC were cut with a vibratome (VT1000S; Leica, Nussloch, Germany). The SOC areas from both sides were then manually excised from the slices. This was performed using a scalpel under visual inspection through a binocular microscope (Fig. 1). After dissection, tissues were stored at −80 °C until further usage. The entire procedure from opening the skull until freezing the SOC sample lasted approximately 30–40 min. The quality of the RNA obtained by this procedure was analysed using the Agilent 2100 Bioanalyser. The ratio of > 1.8 between 28S and 18S rRNA demonstrated only minor, if any, degradation of the RNA during the isolation procedure.

SAGE procedure

Nine SOCs were used for SAGE, which was basically performed as described elsewhere (Jasper *et al*., 2001), with minor modifications introduced. Briefly, poly(A)$^+$ mRNA was isolated using poly dT15 magnetic beads (Dynal, Hamburg, Germany). Double-stranded cDNA was synthesized on the beads and digested with the anchoring enzyme *Nla*III (New England Biolabs, Frankfurt, Germany). After linker-ligation and digestion with the tagging enzyme *Bsm*FI (New England Biolabs), the released linker-tags were blunt-ended and ligated tail to tail. A pre-PCR of 30 cycles was performed on 1 μL of a 1 : 5 dilution of the ligation product to obtain enough starting material for the subsequent large scale amplification PCR (12 cycles) as described previously (Jasper *et al*., 2001). Ten 50 μL PCRs were purified by polyacrylamide gel electrophoresis, extracted with phenol : chloroform and precipitated. The pellets were dissolved in a total of 400 μL LowTE (1 : 10 TE). Large scale PCR was performed on 1 μL of purified pre-PCR product with biotinylated primers resulting in 400 amplification reactions, which were pooled and digested with *Nla*III. The 26-bp ditags were again purified by polyacrylamide gel

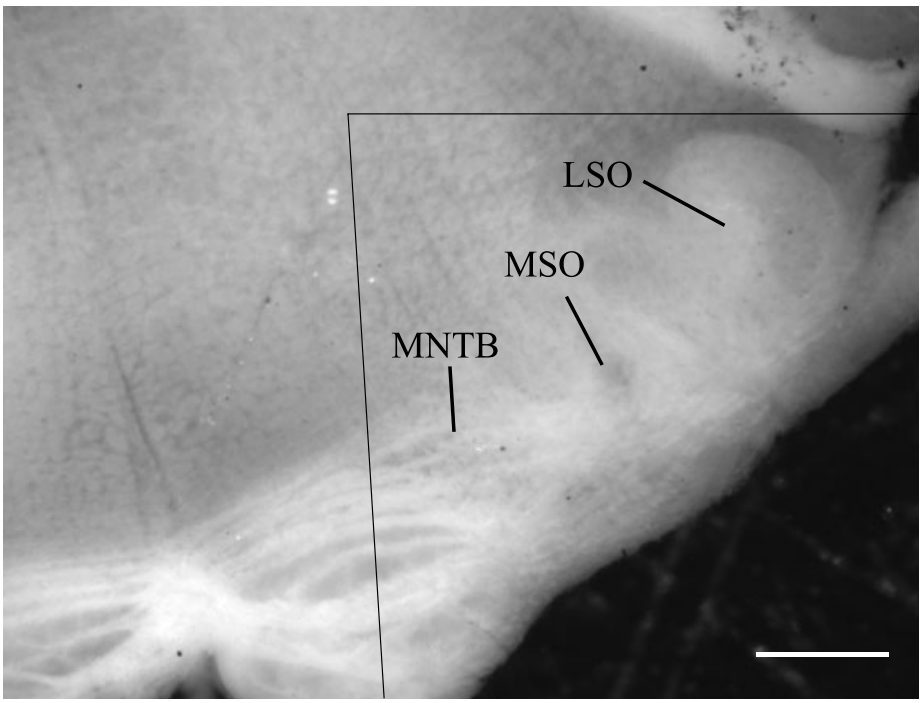

FIG. 1. Tissue section of the rat SOC. (A) An unstained 300-μm-thick brainstem slice is shown depicting the rat SOC area at postnatal day 60. The black lines mark the region that was manually excised and used as the RNA source for SAGE. The major nuclei of the SOC are depicted. LSO, lateral superior olive; MNTB, medial nucleus of the trapezoid body; MSO, medial superior olive. Scale bar, 500 μm.

electrophoresis, and contaminating linker sequences were removed using streptavidin-coated magnetic beads (Roche, Mannheim, Germany). After extraction and precipitation, the pellet was dissolved in 14 μL water and subjected to a 20-μL ligation reaction for concatemerization. After agarose gel electrophoresis, fractions of the desired length were excised, eluted, and cloned into an *Eco*32I-digested pBluescript vector (Stratagene, Heidelberg, Germany) using a previously published protocol (Koehl *et al*., 2003). Inserts were amplified by colony PCR. Sequencing of the PCR products was carried out mainly at the Nano+Bio-Center of the University of Kaiserslautern. Tags were extracted using the SAGE2000 software kindly provided by K. Kinzler. The library contained 6% duplicate ditags, which is well within the acceptable range of 5–25% duplicate ditags in microlibraries (Cheval *et al*., 2000). These duplicates were removed prior to further analysis. Tag annotation was performed using the SAGEmap tag to UniGene mapping (UniGene release #127; ftp://ftp.ncbi.nih.gov/pub/sage/map/Rn/NlaIII/). Gene symbols, aliases, and descriptions were extracted from GeneCards™ (http://thr.cit.nih.gov/cards/index.html). [Note: SAGE data is available at GEO (http://www.ncbi.nlm.nih.gov/geo/) under accession no GSM24492 and at ID-GRAB (http://www.id-grab.de/sage/).]

Data analysis

Reliability scores for tag annotations were provided by the SAGEmap; the score takes into account the different transcript categories in the database (e.g. Refseq sequences, ESTs) and their number matching the respective tag. Annotations with reliability scores < 1 000 500 were excluded from further analysis as these tags match only to expressed sequence tags (ESTs) without a polyadenylation signal (T.O. Suzek, NCBI, personal communication). To compare SAGE libraries, differences were computed pairwise using the *z*-test of the SAGEstat program (Ruijter *et al*., 2002). Only those tags were considered, which had a count greater than four in either of the two libraries, as the count of low abundant tags is not linearly increasing with the library size (Anisimov *et al*., 2002; Stern *et al*., 2003). To compare different functional protein classes, tags were annotated using the gene ontology database. As only < 700 tags were annotated by this procedure, text string searches were performed also. For the tags found in the SOC, only tag counts greater than one were included. To obtain a more global picture of differentially expressed genes, tags only found in hippocampus were included in the analysis if their count was greater than four in the hippocampal SAGE library. For a complete list of the hippocampal transcripts, see Datson *et al*. (2001).

RNA in situ *hybridization*

Probe synthesis

Gene-specific PCR products (see Supplementary material, Table S1) were verified by sequencing and ligated to a T7 promoter. Sense and antisense constructs were obtained by PCR. Digoxigenin (DIG)-labelled cRNA probes were generated using a DIG RNA labelling kit (Roche, Mannheim, Germany) according to the protocol provided. Probes were analysed by gel electrophoresis, and approximately 15–30 ng were applied to every section (final concentration 0.25–0.5 ng/μL).

Histology

Coronal sections of 14-μm thickness were cut in a cryostat, thaw-mounted on poly L-lysine-coated slides, and dried for 1.5 h at room temperature. The protocol for nonradioactive RNA *in situ* hybridization was applied as described previously (Becker *et al*., 2003). Slices were fixed in 4% paraformaldehyde and prehybridization was performed at room temperature in a buffer containing 50% formamide, 4× SSC (600 mM NaCl, 60 mM Na_3citrate, pH 7.0), 10% dextran sulphate, 5× Denhardt's solution, and 200 mg/mL acid-alkali cleaved salmon sperm DNA. After 2 h, the prehybridization buffer was removed and replaced by the same buffer containing the respective probe. Hybridization was performed overnight at 60 °C. Sections were then washed for 30 min at 60 °C in 5× SSC. After RNase A treatment (20 μg/mL) for 15 min at 37 °C, sections were washed for 20 min at 50 °C in 1× SSC. Bound DIG-labelled probes were detected by using an anti-DIG F_{ab} fragment linked to alkaline phosphatase and 4-nitroblue tetrazolium chloride/5-bromo-4-chloro-3-indolylphosphate as the chromogenic substrate. Hippocampal and SOC slices for the same RNA probe were treated in the same way. Generally, the substrate reaction took place for 16 h. No staining was observed in the control slices hybridized with the sense probes.

Photography

Digital images were acquired with a CCD camera system (Hamamatsu C4742-95, 12 bit, 1280 × 1024 pixel, Hamamatsu Photonics, Herrsching, Germany) mounted on a Zeiss brightfield microscope (Axioskop 2, Oberkochen, Germany) and controlled by AnalySIS software (version 3.0, SIS, Münster, Germany). Contrast and brightness were processed using standard image processing software.

Light microscopic immunohistochemistry

Five P60 Sprague–Dawley rats were anaesthetized with a mixture of ketamine HCl (100 mg/mL; WDT, Garbsen, Germany) and xylazine-HCl (Rompun; 20 mg/mL; Bayer, Leverkusen, Germany) at 0.1 mL/100 g body weight. The animals were perfused transcardially with saline, followed by the fixative consisting of 4% paraformaldehyde in 0.12 M phosphate buffer, pH 7.2. After perfusion, brains were removed, postfixed for 1 h at 4 °C, rinsed three times in phosphate buffered saline, and stored overnight at 4 °C. For peroxidase immunohistochemistry, brain coronal and sagittal sections (30-μm thick) were cut in cold phosphate buffered saline using a Vibratome (Leica, Vienna, Austria). Slices were incubated for 1 h in phosphate buffered saline containing 10% normal goat serum and then with the primary antibody to the $P2X_6$ subunit (Rubio & Soto, 2001) in phosphate buffered saline (0.9 mg/mL) overnight at 4 °C and processed using the avidin-biotin-peroxidase system (Vectastain kit; Vector Laboratories, Burlingame, USA). Antibody binding was visualized using 3–3′-diaminobenzidine tetrahydrochloride (DAB) and nickel chloride (DAB-Ni substrate kit for peroxidase, Vector Laboratories, Burlingame, CA). Controls were performed either by omitting the primary antibody or by preincubating the primary antibody with the corresponding fusion protein (final concentration; 15 mg/mL) at 4 °C for 24 h and then by following the above procedure. No positive staining was observed in the control slices. Sections were analysed and digital images were acquired with a CCD camera system (MicroPublisher 5.0, 8 bit, 2.560 × 1.920 pixel) mounted on a Zeiss Axioskop brightfield microscope and controlled by QCapture software (Quantitative Imaging Corporation, Burnaby, Canada). Contrast and brightness were processed using a standard image processing software (Adobe Photoshop 5.0, Adobe Systems, San Jose, California).

Results

Generation of a SOC SAGE library from young-adult rats

To obtain a catalogue of expressed genes in the SOC of young-adult rats, we constructed a SAGE library from P60 animals. A total of 31 035 tags were sequenced. They represented 10 473 unique tags of which 7093 (67.7%) had a tag count of one. A full description of tag abundance levels is accessible via the publicly available databases ID-GRAB (http://www.id-grab.de) and GEO (http://www.ncbi.nlm.nih.gov/geo/ GEO number GSM24492). Among the ten most abundant tags, five tags were derived from mitochondrial genes (counts between 2616 and 161), three were derived from genes encoding glial proteins (myelin basic protein, count 566; proteolipid protein, count 247; SPARC-like 1, count 126), one was derived from the gene encoding tubulin alpha 1 (count 125), and one tag (count 134) could not be mapped to any known gene or EST (data not shown). Concerning all 31 035 tags, 65% (20 302 tags) corresponded to known genes or ESTs, 16.5% (5110 tags) corresponded to mitochondrial genes and 17% (5296 tags) had no annotation. With respect to the 10 473 unique tags, 65% (6759 tags) corresponded to known genes or ESTs, 35% (3679 tags) had no annotation and 0.3% (35 tags) corresponded to mitochondrial genes (data not shown).

General comparison between SOC library and hippocampus library

To identify genes that may play important roles in SOC function, we compared our data with a publicly available SAGE library from the rat hippocampus (GEO number GSM1679 Datson *et al*., 2001) which, at present, represents the only other large SAGE library obtained from normal rat brain and contains 28 748 unique tags. Our premise was that those genes that are significantly more highly represented in the SAGE library of the SOC compared to the hippocampus might play an important role in this tissue. From a total of 2613 unique tags with a count greater than four in either of the two libraries, 543 (21%) were statistically more highly represented in the SOC at a P-value < 0.05, 244 (9%) at a P-value < 0.001, and 97 (4%) at a P-value $< 10^{-5}$ (Table 1). From the 299 tags with no annotation and a count greater than four, 35 (11.7%) were statistically more highly represented in the SOC at a P-value < 0.05, 17 tags (5.7%) at a P-value < 0.001 and nine (3%) at a P-value $< 10^{-5}$ (data not shown). In the hippocampus, 329 (13%) tags were over-represented at a P-value < 0.05, 59 (2%) at a P-value < 0.001, and 27 (1%) at a P-value $< 10^{-5}$ (Table 1).

Comparison of specific functional protein classes

Energy metabolism and myelination

Two functional gene classes were strikingly up-regulated in the SOC. One class represented genes whose products are involved in energy metabolism, such as glucose transport, glycolysis, the citrate cycle, and the respiratory chain (Table 2). Twenty-five tags of the identified 42 genes were significantly more highly represented in the SOC compared to the hippocampus. By contrast, only four transcripts were more highly represented in the hippocampus. The second class of transcripts comprised genes encoding proteins of the myelin sheaths. Seven out of 11 genes were significantly up-regulated in the SOC and an additional tag, derived from the gene encoding the potassium channel Kir4.1, was found four times in the SOC library, yet not at all in the hippocampus (Supplementary material, Table S2).

Neuronal membrane proteins

As membrane proteins define many neuronal properties, we next analysed plasma membrane receptors, channels, transporters, and vesicular transporters. In general, genes encoding plasma membrane receptors showed a low expression with an average of 3.2 counts/tag (tags with a count of one were not included). A total of 29 receptor genes were identified in the SOC with a tag count greater than one (Table 3). In addition, in the hippocampus, 14 tags for receptors were identified with a count grater than four that were not present in the SOC (Table 3, transcript numbers 5, 14, 36–41, 43, 45–49). Thirteen of the tags in the SOC represented a total of 11 different neurotransmitter receptors (Table 3, transcript numbers 1–4, 6–13, 15). Among them, the largest family was the glutamate receptor family with three gene members. Two transcripts, one encoding the neurotensin receptor Ntsr2 and the other one the purinergic receptor subunit $P2X_6$, were significantly more highly represented in the SOC than in the hippocampus. Five tags for neurotransmitter receptor genes were significantly over-represented in the hippocampus, including transcripts for *Gria2* and *Htr5b* (Table 3, transcript numbers 1, 5, 7, 8 and 36).

Genes encoding plasma membrane ion channels and transporters displayed an increased expression level compared to those encoding plasma membrane receptors. We found averages of 12 counts/tag and 7.9 counts/tag, respectively, again omitting all the tags with a count of one (Table 4). Among the 16 detected channels in the SOC, six were significantly more highly represented in the SOC library (Table 4, transcript numbers 3, 5, 6, 8, 14, 15). Among them were *Kcnc1* and *Scn1b*, encoding the voltage gated potassium channel Kv3.1 and the sodium channel beta-1 subunit, respectively. In addition, two transcripts with a tag count lower than five were detected in the SOC, yet not in the hippocampus SAGE library (Table 4, transcript numbers 10, 13). In the hippocampus, five tags were significantly more highly represented (Table 4, transcript numbers 12, 63, 64, 66, 67). Among them were *Cacna2d1* and *Kcnd2*, encoding a voltage gated calcium channel and a voltage gated potassium channel, respectively. The largest gene family in the SOC was formed by the potassium channels with seven identified

TABLE 1. Quantitative assessment of differential gene expression between SOC and hippocampus

	Tags with count > 4	No annotation	Differentially regulated	Over-represented in SOC			Over-represented in hippocampus		
				$P < 0.05$	$P < 0.001$	$P < 10^{-5}$	$P < 0.05$	$P < 0.001$	$P < 10^{-5}$
Counts	2613	299	872	543	244	97	329	59	27
Percentages	100	11	34	21	9	4	13	2	1

Only tags with counts greater than four in the SOC library were analysed for this table. Data for the hippocampus SAGE library were taken from Datson *et al*. (2001). The column 'Tags with a count > 4' summarizes all tags with counts higher than four in either of the two libraries, 'No annotation' summarizes all tags that were not annotated by the NCBI. P-values were computed by the z-test using the SAGEstat program (Ruijter *et al*., 2002).

TABLE 2. Comparative quantitative analysis between SOC and hippocampus of 42 genes involved in energy metabolism

Transcript number	Tag sequence	Gene description	Gene name	SOC	Hippocampus	Function
1	AGAAGGACCT	Facilitated glucose transporter, member 1	*Slc2a1*	2	0	A
2	TTACTGTAGT	Facilitated glucose transporter, neuronal member 2	*Slc2a3*	8*	3	A
3	TTTTGTAATT			1	2	A
4	CAGTCTCGCC	Facilitated glucose transporter, member 8	*Slc2a8*	2	0	A
5	CCTACTAACC	Aldolase A	*Aldoa*	12	62*	B
6	TCTGAGGATG	Aldolase C	*Aldoc*	46**	14	B
7	TGATCAGTCT	Enolase 1, alpha	*Eno1*	24**	10	B
8	TCCCACAGTT	Enolase 2, gamma	*Eno2*	5*	1	B
9	AGGATTGAAG			1	36**	B
10	GCCTCCAAGG	Glyceraldehyde-3-phosphate dehydrogenase	*Gapd*	64*	99	B
11	CCGCCTGGAG			0	7	B
12	GGCTCAGCCT	Glucose phosphate isomerase	*Gpi*	24	39	B
13	CCAAGGAAAA	Lactate dehydrogenase A	*Ldha*	5	37*	B
14	TGATAATGAG	Lactate dehydrogenase B	*Ldhb*	61**	27	B
15	GCTTCTCAGT	Phosphofructokinase	*Pfkm*	3	7	B
16	TTCCAGCTGC	Phosphoglycerate mutase 1	*Pgam1*	19	33	B
17	GAAATAACGG	Phosphoglycerate kinase 1	*Pgk1*	37**	20	B
18	TAGATGACTT	Pyruvate kinase	*Pkm2*	19**	10	B
19	CTTCTGATAA	Triosephosphate isomerase 1	*Tpi1*	2	23*	B
20	TTTGGTTTAA	ATP citrate lyase	*Acly*	8*	5	C
21	CAACTGTATT	Aconitase 2	*Aco2*	15	24	C
22	TGCAATAATG	NAD(H)-specific isocitrate dehydrogenase 1	*Idh1*	5*	1	C
23	TGAGCAATTT	NAD(H)-specific isocitrate dehydrogenase 2	*Idh2*	3	0	C
24	TCTGGGTCAT	NAD(H)-specific isocitrate dehydrogenase, 3α	*Idh3a*	4	3	C
25	AATTACTACT			2	1	C
26	TAAAAATAAA	NAD(H)-specific isocitrate dehydrogenase, 3β	*Idh3b*	10**	3	C
27	TATGAAATTT	Fumarate hydratase 1	*Fh*	2	2	C
28	TTGTTAGTGC	Malate dehydrogenase 1	*Mdh1*	89**	112	C
29	GAGAGGAAGG			1	0	C
30	ACGTAAAAAA			2	19	C
31	TCATTGAACT	Malate dehydrogenase 2	*Mdh2*	14*	8	C
32	AGTATAACTA	Succinate dehydrogenase complex, subunit A, flavoprotein	*Sdha*	4	0	C
33	CATTTATTCA			1	2	C
34	AGTATAACTA			4	0	C
35	AACAAGGAGT			3	3	C
36	CATTTATTCA			1	2	C
37	TTTTAGAATG	Succinate-CoA ligase, GDP-forming, a	*Suclg1*	11*	12	C
38	AATAAAAGTT	Mitochondrial ATP synthase subunit alpha, 1	*Atp5a1*	36**	22	D
39	GCTGGCCCCG			2	0	
40	TAGGCCACAC	Mitochondrial ATP synthase subunit beta	*Atp5b*	33*	48	D
41	GACAACGCCA	Mitochondrial ATP synthase subunit gamma 1	*Atp5c1*	9*	9	
42	GAGGGCTTCC	Mitochondrial ATP synthase subunit delta	*Atp5d*	5	8	D
43	TGGGCACCTG	Mitochondrial ATP synthase subunit epsilon	*Atp5e*	20*	23	D
44	TGATACAGAG	Mitochondrial ATP synthase subunit b, isoform 1	*Atp5f1*	2	3	D
45	ATTTAAAATA			2	1	
46	CCAGTCCTGG	Mitochondrial ATP synthase subunit c, isoform 1	*Atp5g1*	23**	8	D
47	GTTCTTCCGT	Mitochondrial ATP synthase subunit c, isoform 2	*Atp5g2*	3	15	D
48	GAAATATGTG	Mitochondrial ATP synthase subunit c, isoform 3	*Atp5g3*	68**	44	D
49	ACTTAGTTGT	Mitochondrial ATP synthase subunit F6	*Atp5j*	14	38	D
50	CGGGATCTGC	Mitochondrial ATP synthase O subunit	*Atp5o*	19**	16	D
51	TTAATAAATG	Cytochrome *c* oxidase, subunit 4a′	*Cox4a*	51**	16	D
52	CATCCTTGAT	Creatine kinase	*ckb*	87**	56	E
53	GATAAAACCA	Mitochondrial adenine nucleotide translocator 4	*Slc25a4*	32*	41	F
54	GATAAAAAAA			2	3	
55	TTGTATAATA	Mitochondrial adenine nucleotide translocator 5	*Slc25a5*	15**	10	F

The table lists a selected number of genes that are involved in energy metabolism. Data for the hippocampus SAGE library were taken from Datson *et al*. (2001). Tags below a count of two were not included in the list. Genes are categorized into functional classes; within a functional class, they are listed in alphabetic order of the gene symbols. Transcript number represents an arbitrary numbering of tags for easier citation in the text. Asterisks denote tags which are significantly more highly represented in either of the two libraries as calculated by the *z*-test (Ruijter *et al*., 2002): *$P < 0.05$; **$P < 0.001$. A, glucose transport; B, glycolysis; C, tricarbon acid cycle; D, respiratory chain; E, energy transduction; F, ATP translocation.

members (Table 4, transcript numbers 6–12), followed by gap junction channel subunits with four members (Table 4, transcript numbers 2–5) and sodium channels with three members (Table 4, transcript numbers 13–15).

Forty-three unique tags were identified in the SOC for transcripts encoding plasma membrane transporters or vesicular transporters. Of these, 13 tags were significantly more highly represented in the SOC library (Table 4, transcript numbers 18, 21, 22, 34, 39, 41, 49, 52, 53, 56, 58, 59, 62). Among them were transcripts encoding the vesicular amino acid transporters VIAAT and VGLUT2. Another ten tags with a count lower than five in the SOC were not present in the hippocampus SAGE library (Table 4, transcript numbers 29, 33, 35,

TABLE 3. Comparative quantitative analysis between SOC and hippocampus of 44 genes encoding plasma membrane receptors

Transcript number	Tag sequence	Gene description	Gene name	SOC	Hippocampus
1	TGGCCCAACA	Bradykinin receptor B1	*Bdkrb1*	2	60**
2	TTTATATAAA	Cholinergic receptor, muscarinic 3	*Chrm3*	3	4
3	CTGCCAAACA	GABA B receptor, 1	*Gabbr1*	2	6
4	AAAACAGGAT			1	1
5	TTTTCTGAGC			0	10*
6	GTATCGATTT	G-protein coupled GABA-B receptor 2	*Gpr51*	3	4
7	GAAATACTAT	Glutamate receptor, ionotropic, 2	*Gria2*	2	14*
8	TGTACTATGT			1	19*
9	GATTCTGGGT	Glutamate receptor, ionotropic, kainate 4	*Grik4*	2	0
10	TATGTACACA	Glutamate receptor, ionotropic	*Grinl1a*	5	5
11	TCTGTCTTTA	Glycine receptor, alpha 1 subunit	*Glra1*	4	3
12	CTCTGCTGCC	Histamine receptor H3	*Hrh3*	2	4
13	CATTTGGCTA	Neurotensin receptor 2	*Ntsr2*	12*	12
14	TAAACTTACT			0	5
15	GACACAGTAG	Purinergic receptor P2 × 6	*P2rx6*	5**	0
16	TACTTGTGTT	Stromal cell derived factor receptor 1	*Sdfr1*	8	39
17	TCTGTAGCCC	Thyroid hormone receptor alpha	*Thra*	7	52*
18	TGACAGGAGT	Fibroblast growth factor receptor 2	*Fgfr2 f*	6**	1
19	GAAGAGAATC	Ig-Hepta G protein-coupled hepta-helical receptor Ig-Hepta	*Gprhep*	5**	0
20	CACACAGATA	Glucagon receptor	*Gcgr*	4	1
21	CATACACATA	Growth hormone receptor	*Ghr*	3	0
22	AATTACTGAC	Transient receptor protein 1	*Trrp1*	3	1
23	TGGCCATCTT			1	0
24	GTCCAGACAC	Protein tyrosine phosphatase, receptor type, A	*Ptpra*	3	1
25	AAAGGCAAAG	Endothelial differentiation, lysophosphatidic acid G-protein-coupled receptor, 2	*Edg2*	2	2
26	AAGACTCATA	Glial cell line derived neurotrophic factor family receptor alpha 1	*Gfra1*	2	1
27	TTTTATTGCA	Gonadotropin-releasing hormone receptor	*Gnrhr*	2	7
28	AAACTTAGCA	G-protein-coupled receptor 37	*Gpr37*	2	3
29	AAAATAAAAG	Killer cell lectin-like receptor subfamily B member 1B	*Klrb1b*	2	1
30	CAGGCAAGCC	Nogo-66 receptor homolog 2	*Ngrh2*	2	3
31	ATTGAGAACA	Protein tyrosine phosphatase, receptor-type, Z polypeptide 1	*Ptprz1*	2	4
32	CTCAATAAAT	Thromboxane A2 receptor	*Tbxa2r*	2	1
33	CCCTTATAGA	Transferrin receptor	*Tfrc*	2	2
34	TTACTAACAC	Tyrosine kinase receptor 1	*Tie1*	2	0
35	TGGTTTACTC	Neuronal pentraxin receptor	*Nptxr*	1	31*
36	TAATGGAAGG	Serotonin-receptor 5B	*Htr5b*	0	24*
37	TCTATTGTCT	Cannabinoid receptor 1	*Cnr1*	0	19*
38	GCCTTTGTGG	Neurotrophic tyrosine kinase, receptor, type 2	*Ntrk2*	0	15*
39	ATACAGGGAC	Adenosine A1 receptor	*Adora1*	0	10*
40	GAAGGGTATT	Coxsackie virus and adenovirus receptor	*Cxadr*	0	9
41	GTCTTTGTCA	Neurotrophic tyrosine kinase, receptor, type 2	*Ntrk2*	0	7
42	TCTTTCTAAA	Fibroblast growth factor receptor 1	*Fgfr1*	1	7
43	AGCATCAAGG	Cadherin EGF LAG G-type receptor 2	*Celsr2*	0	6
44	TTCTCTCTCT	Putative G protein-coupled receptor snGPCR32	*Edg7*	1	6
45	ACCAGCTCTC	Glutamate receptor, ionotropic, NMDA 1	*Grin1*	0	6
46	TCTCTAATTG	Protein tyrosine phosphatase, N 2	*Ptprn2*	0	6
47	TCATTTTAAC	Protein tyrosine phosphatase Z 1	*Ptprz1*	0	6
48	CAGGCAAAGC	Chemokine (C-C motif) receptor 9	*Ccr9*	0	5
49	GGGTGGGAAG	Protein tyrosine phosphatase, F	*Ptprf*	0	5

The table lists the genes that encode plasma membrane receptors. Data for the hippocampus SAGE library were taken from Datson *et al*. (2001). Tags below a count of two were not included in the list except in cases where several tags had the same gene annotation to account for low expression of genes encoding membrane proteins. Genes encoding neurotransmitter receptors are first listed in alphabetic order, then other receptors in descending order of tag count in the SOC. Finally, genes with a tag count greater than four are listed that encode receptors restricted to the hippocampus. Transcript number represents arbitrary numbering of tags for easier citation in the text. Asterisks denote tags which are significantly more highly represented in either of the two libraries as calculated by the *z*-test (Ruijter *et al*., 2002). $*P < 0.05$; $**P < 0.001$.

40, 43–47, 50). In the hippocampus, four tags were significantly over-represented (Table 4, transcript numbers 19, 23, 51, 65) and an additional four tags were restricted to the hippocampal library (Table 4, transcript numbers 20, 31, 68, 71). Among them was the transcript encoding the noradrenalin neurotransmitter transporter 2. The largest gene family with six members in the SOC encoded subunits of the Na^+/K^+ ATPase, followed by the glucose transporter family Slc2 and the cation chloride cotransporter family Slc12 with three members each.

Miscellaneous neuronal proteins

Finally, we searched the SOC SAGE library for other genes with important roles in neuronal function (Table 5). Among them were genes encoding the Ca^+-binding proteins calbindin 1, calcium binding protein 1 and parvalbumin. The latter was significantly more highly represented in the SOC than in the hippocampus. Four other genes that were significantly more highly represented in the SOC library encoded the NMDA receptor glutamate binding chain GrinA, the glutamine

TABLE 4. Comparative quantitative analysis between SOC and hippocampus of 62 genes encoding plasma membrane ion channels and selected transporters

Transcript number	Tag sequence	Gene description	Gene name	SOC	Hippocampus
1	ACAAATGCTT	Nucleotide-sensitive chloride channel 1 A	*Clns1a*	3	1
2	TGCTCGGGAG	Connexin 43	*Gja1*	12	42
3	TTAAAAAAAA	Connexin 40	*Gja5*	13*	15
4	TTTGCTGTGA	Connexin 36	*Gja9*	2	1
5	TCAGTGGGGA	Connexin 32	*Gjb1*	5**	0
6	AAATAAATTT	Potassium voltage gated channel Kv3.1	*Kcnc1*	6*	3
7	TTACTAACTG	Potassium voltage gated channel Kv3.2	*Kcnc2*	2	3
8	CCCCTCCCCA	Potassium voltage gated channel Kv3.3	*Kcnc3*	7*	3
9	TTTTTTATAT	Potassium voltage gated channel Kv12.2	*Kcnh3*	2	2
10	ACTATGCAGG	Glial ATP-dependent potassium channel Kir4.1	*Kcnj10*	4	0
11	GCAGATTGCA	2-pore domain potassium channel TWIK-1	*Kcnk1*	7	8
12	GTGGCTCACA	2-pore domain potassium channel TWIK-2	*Kcnk6*	62	768**
13	TTGGAAAATG	Sodium channel, voltage-gated, type I, alpha	*Scn1a*	3	0
14	AAATAAAGAT	Sodium channel beta-1 subunit	*Scn1b*	56**	7
15	CCCAGCACTT	Sodium channel beta-4 subunit	*Scn4b*	5*	1
16	ATGAAGCCAG	Voltage-dependent anion channel 1	*Vdac1*	4	5
17	TAGCTGTAAT	ATPase, Na^+/K^+ transporting, alpha 1	*Atp1a1*	3	6
18	TGTACTTGAA	ATPase, Na^+/K^+ transporting, alpha 2	*Atp1a2*	43**	46
19	GCCCCCCTCT	ATPase, Na^+/K^+ transporting, alpha 3	*Atp1a3*	5	99**
20	TCTTCCCTGC			0	6
21	TTCTAGCATA	ATPase Na^+/K^+ transporting beta 1	*Atp1b1*	87**	77
22	GTGGAAGAAT			10*	6
23	AACGAGGAGA			0	39**
24	GAAGAAACAG	ATPase, Na^+/K^+ transporting, beta 3	*Atp1b3*	6	5
25	GGATACGTTT	ATPase, Ca^{++} transporting, plasma membrane 2	*Atp2b2*	2	2
26	TGTTCACTAT	ATPase, Ca^{++} transporting, plasma membrane 3	*Atp2b3*	2	14
27	GATCATATCT	Choline transporter-like protein	*Ctl1*	3	3
28	ATCTGTTTAT			3	1
29	TGCTCGCAAT			3	0
30	AAGATGTGTT	GABA transporter protein	*Gabt1*	10	16
31	GGTCTGGGAG	Excitatory amino acid transporter EAAT3	*Slc1a1*	0	9
32	GTGAACGTTC			2	1
33	AGAAGGACCT	Facilitated glucose transporter, member 1	*Slc2a1*	2	0
34	TTACTGTAGT	Facilitated glucose transporter, member 3	*Slc2a3*	8*	3
35	CAGTCTCGCC	Facilitated glucose transporter, member 8	*Slc2a8*	2	0
36	ACAGTGAAGG	Activators of dibasic and neutral amino acid transport, member 2	*Slc3a2*	2	3
37	CCAGGACAGT	Anion exchanger AE3	*Slc4a3*	4	1
38	CCCAGCTTTT	Sodium iodide symporter	*Slc5a5*	2	1
39	CATTTTGTTC	Sodium-dependent vitamin transporter	*Slc5a6*	6**	0
40	CTTCTGCAGA	System y + basic amino acid transporter	*Slc7a1*	2	0
41	TTGTTTATTG	System y + cationic amino acid transporter	*Slc7a10*	7**	0
42	TACAAAGCCA	Sodium/hydrogen exchanger	*Slc9a1*	3	1
43	TATATTATTG	Ileal apical sodium-dependent bile acid transporter	*Slc10a2*	2	0
44	GACACGTTGC	Na-K-Cl-cotransporter NKCC1	*Slc12a2*	1	0
45	AAAACAGACT			1	0
46	ATGCTTTTGA			1	0
47	AGATGAAATA	Thiazide-sensitive Na-Cl transporter NCC[a]	*Slc12a3*	2	0
48	TCCATCCAGG	Neuronal K-Cl cotransporter KCC2	*Slc12a5*	3	3
49	ATTTCTGATA	Na/dicarboxylate cotransporter 3	*Slc13a3*	9**	0
50	TAGAAAAATG	Monocarboxylate transporter 1	*Slc16a1*	3	0
51	CCAACAAGAA	Monocarboxylate transporter 7	*Slc16a6*	25	131**
52	TGACCATAAC	Differentation-associated Na-dependent inorganic phosphate cotransporter vGLUT2	*Slc17a6*	7*	2
53	TTCATCTGTC	Sodium/phosphate transporter GLVR1	*Slc20a1*	13**	6
54	CGTTAAAATA	Organic anion transporter 5	*Slc21a5*	3	1
55	ATATAAAGTG	Na-independent organic anion transporter D	*Slc21a11*	4	1
56	CTGAGCCTTG	Fatty acid transport protein	*Slc27a1*	11*	11
57	AGGCTTTATG	Zinc transporter 1	*Slc30a1*	4	2
58	CCCTAGACAT	Vesicular inhibitory amino acid transporter VIAAT	*SLc32a1*	5**	0
59	TGATTTCAAT	Na-coupled neutral amino acid transporter SNAT2	*Slc38a2*	14**	1
60	GAGTCAGCAT	Na-coupled neutral amino acid transporter SNAT3	*Slc38a3*	3	2
61	GAGGAAACCA			1	2
62	TGAATATGTC	Na-Cl-transporter X3	*Xtrp3*	12*	12
63	CTGCATCATC	Calcium channel, voltage-dependent, $\alpha 2/\delta$ 1	*Cacna2d*1	0	18*
64	TGAACAGACA	Sodium channel beta 3 subunit	*Scnb3*	0	17*
65	TAGTGTTTTC	ATPase, Ca^{++} transporting, plasma membrane 1	*Atp2b1*	1	16*
66	AGTGGCTAAT	Chloride channel 2	*Clcn2*	0	15*
67	GGAGCCCTGA	Potassium voltage gated channel Kv4.2	*Kcnd2*	0	13*

TABLE 4. Continued

Transcript number	Tag sequence	Gene description	Gene name	SOC	Hippocampus
68	TTCTCTGTGT	Noradrenalin neurotransmitter transporter 2	*Slc6a2*	0	7
69	AGTCCTTTTA	Chloride channel 3	*Clcn3*	0	6
70	TTCTGTGTGG	Excitatory amino acid transporter EAAT4	*Slc1a6*	1	5
71	AGTACGTTCT	Orphan neurotransmitter transporter v7–3	*Slc6a15*	0	5

The table lists the genes that encode plasma membrane ion channels and selected transporters. Data for the hippocampus SAGE library were taken from Datson *et al.* (2001). Tags below a count of two were not included in the list except in cases where several tags had the same gene annotation to account for low expression of genes encoding membrane proteins. Genes encoding plasma membrane channels are first listed in alphabetic order of the gene symbols, then selected transporters again in alphabetic order. Finally, transcripts with a tag count greater than four are listed that encode channels and transporters restricted to the hippocampus. Transcript number represents arbitrary numbering of tags for easier citation in the text. Asterisks denote tags which are significantly more highly represented in either of the two libraries as calculated by the *z*-test (Ruijter *et al.*, 2002). $*P < 0.05$; $**P < 0.001$. [a], not detected by RNA *in situ* hybridization (Becker *et al.*, 2003).

synthetase Glns, the glutamate dehydrogenase Glud1, and the synaptosomal-associated protein Snap25. In the hippocampus, the genes encoding the Cl1ba protein, complexin 2, hippocalcin, neurogranin, Sip30, somatostatin, Snap91 and Sparc showed a significantly higher expression level.

Confirmation of SAGE data

In order to validate our SOC SAGE data, we performed several independent analytical tests. First, we analysed the data in relation to 32 cytosolic proteins, which we have recently identified in a proteomic approach using mass spectrometry in the SOC of P60 rats (Nothwang *et al.*, 2003). Each of these proteins had corresponding tags in the SAGE library (Supplementary material, Table S3); thus, we obtained matching information about proteins and transcripts. Second, we performed RNA *in situ* hybridization experiments in the SOC and hippocampus to assess whether the SAGE data were reflected by histological results, both in terms of the anatomical structure and the expression level. cDNA probes corresponding to 11 different tags with various abundance (ranging from 103 to four), all of them being over-represented in the SOC, were employed: *Snap25* (103 tags), *Scn1b* (56 tags), *AldoC* (46 tags), *Glud1* (40 tags), *S100b* (36 tags), *GrinA* (21 tags), *Sc2* (19 tags), *Calb1* (eight tags), *Slc2a3* (eight tags), *P2rx6* (five tags), and *Trrp1* (four tags). In addition, expression of one gene was analysed that was equally present in both libraries (*Ppia*) 23 tags, and one gene that was only present in the hippocampal SAGE library (*Camk2a*) (33 tags). Most genes were expressed throughout the SOC, with the strongest expression often occurring in the MNTB and the MSO (Fig. 2; see Supplementary material, Fig. S1). A notable exception was *Calb1* for which we found a strong expression restricted to the MNTB (Fig. 2G). In the hippocampus, gene expression was detected mostly in the pyramidal layer of the CA1–CA3 regions and the granular cell layer of the dentate gyrus (DG) (Fig. 2; see Supplementary material, Fig. S1). Only *AldoC* and *Slc2a3* were also abundantly expressed in the molecular layer (Fig. 2D; see Supplementary material, Fig. S1, J). In general, signal intensities, judged by eye inspection, were in good agreement with the respective tag count in the SAGE library. However, due to the differences in labelling and hybridization efficiency of the probes, an exact comparison of expression levels between different genes is difficult. For example, labelling obtained with the *Slc2a3* cDNA probe, which was represented by only eight tags in the SAGE library, was stronger than labelling obtained with the *Glud1* or the *S100b* probe (40 and 36 tags, respectively) (see Supplementary material, Fig. S1, D, E and J).

For the great majority of genes, their broad expression in the SOC and their restricted expression in the hippocampus, namely in the CA and DG regions, was in accordance with a higher tag count seen in the SOC than in the hippocampus. The only exception was *Scn1b*, where the *in situ* hybridization results indicated a smaller difference in the expression level than was predicted by the comparison of tag counts (180 in the SOC and nine in the hippocampus when normalized to 100 000 tags) (see Supplementary material, Fig. S1, B). In addition, for most genes, such as *Scn1b*, *AldoC*, *S100b*, *GrinA*, and *Sc2*, the expression signals were stronger in individual SOC neurons than in hippocampal neurons, indicating that the higher expression value is also manifest at the single-cell level. *Ppia*, which, according to SAGE, is equally abundant in the SOC and the hippocampus, displayed a rather uniform labelling in both brain regions, thus complying with the SAGE data (see Supplementary material, Fig. S1, F). *Camk2a*, which was found only in the hippocampus SAGE library, showed a strong staining in the pyramidal layer and the DG, whereas in the SOC, only the MNTB was weakly stained (see Supplementary material, Fig. S1, M).

An interesting finding was the detection of the purinergic receptor gene *P2rx6* in the SOC SAGE library (five counts), because this neurotransmitter receptor had not been characterized as yet in the SOC. To further analyse its expression, RNA *in situ* hybridization was performed. A strong expression signal was observed in most SOC nuclei, e.g. the MNTB, the MSO, and the LSO (Fig. 3A). In the hippocampus, a high expression was observed in the CA and DG regions (Fig. 3B). To validate these data, immunohistochemistry was performed. This confirmed the presence of the $P2X_6$ receptor subunit in the SOC. Strong signals were observed in the MNTB and moderate signals in the other nuclei (Fig. 3C). Analysis at higher resolution resulted in the localization of the $P2X_6$ subunit in SOC neurons, as shown by the intense labelling of the somata in the MTNB and LSO (Fig. 3E–G). $P2X_6$ subunits do not form functional homomeric receptors in expression systems. However, they form functional heteromeric receptors when coexpressed with $P2X_4$ subunits (Collo *et al.*, 1996; Khakh, 2001; North, 2002). We corroborated the coexpression by RNA *in situ* hybridization results, which demonstrated an overlapping expression pattern of $P2X_4$ subunits with $P2X_6$ subunits in the SOC (Fig. 3H).

Discussion

SAGE methodology

To generate a comprehensive list of genes that are expressed in the adult rat SOC, we have performed SAGE. This technique permits a

TABLE 5. Comparative quantitative analysis between SOC and hippocampus of genes encoding selected proteins important for neuronal function

Transcript number	Tag sequence	Gene description	Gene name	SOC	Hippo-campus
1	AAATAAAGTC	Agrin	*Agrn*	6	5
2	GACCAGCAAC	Amphiphysin	*Amph1*	0	5
3	TCTGCCCCGA	Calcium binding protein 1	*Cabp1*	3	6
4	TGTTCCAGAT	Calbindin 1	*Calb1*	8	10
5	CAGCTTGGTG	Calmodulin 1	*Calm1*	0	7
6	TCTCCAACTT			2	10
7	TTGCTGTTGA	Calmodulin 2	*Calm2*	9	35
8	CCCGTTCTCC	Calmodulin 3	*Calm3*	2	18
9	GGCTGGATGG	Cholecystokinin	*Cck*	0	9
10	CTACAGTTCC	CL1BA protein	*CL1BA*	0	15*
11	ACTCCTGTCA	Clathrin, light polypeptide	*Cltb*	5	9
12	TTCAAGAAGT	Complexin 2	*Cplx2*	0	15*
13	CCTCTGTTTG	Cysteine string protein	*Csp*	11	14
14	GTGACCTGTC			3	11
15	TGTGTCTCCA	Dopa decarboxylase	*Ddc*	3	4
16	TGGAATCAAG	Gephyrin	*Gphn*	1	5
17	TATAGTATGT	Glutamine synthetase 1	*Glns*	45**	38
18	TCACTAAAGC			4	5
19	ATTAACTTGG	Glutamate dehydrogenase 1	*Glud1*	36**	34
20	CTGCTGTAAT			4	4
21	TTTCAGGGGA	NMDA receptor glutamate-binding chain	*Grina*	21**	12
22	ATTAAATGAG	Neuronal immediate early gene homer 1	*Homer1*	4	0
23	ACAGTTCCAG			3	2
24	CGCCACACGG	Hippocalcin	*Hpca*	0	45**
25	TGGACACTCA	Neurochondrin	*Ncdn*	30	90
26	GAAAAAATGT	Nerve growth factor receptor associated protein 1	*Ngfrap1*	3	4
27	CATTCAAAAA	Neuropeptide Y	*Npy*	0	6
28	CAGCTCTGCC	Neurogranin	*Nrgn*	2	139**
29	TTACCATACT			0	54**
31	TGACCTATAG	Neuropilin	*Nrp*	0	9
32	CCCCATCTCA	Parvalbumin	*Pva*	18**	2
33	CCCATAATCC	Synaptic glycoprotein SC2	*Sc2*	19**	7
34	GTATTGACAA	Secretogranin 2	*Scg2*	3	16
35	CATTTTACAT	Secretory granule neuroendocrine protein 1	*Sgne1*	2	6
	TCTTCGTGAC	SNAP25 interacting protein 30	*Sip30*	40	185**
36	GCACCCCGGG	Somatostatin	*Sst*	0	10*
37	TATATTAAAT	Synaptosomal-associated protein 25 kDa	*Snap25*	94**	70
38	TTTATTAAAT			9*	4
39	TCTGCCCTCT	Synaptosomal-associated protein, 91 kDa	*Snap91*	8	42*
40	GAACATTGCA	Secreted acidic cysteine rich glycoprotein	*Sparc*	1	29*
41	TCTGCTAAAA	Syntaxin 7	*Stx7*	1	5
42	GTCAAACCAG	Synaptic vesicle glycoprotein 2 a	*Sv2a*	1	5
43	AGTTGGAAAC	Synaptic vesicle glycoprotein 2 b	*Sv2b*	10	28
44	CTCTGTGTGG	Synaptic vesicle protein 2C	*Sv2c*	4	0
45	CCGCTATAAC	Synapsin 2	*Syn2*	1	5
46	GAATTTTTAC	Synaptojanin 1	*Synj1*	2	4
47	AAAATAAACT	Synaptotagmin 2	*Syt2*	2	0
48	CCCTGGTCCC	Synaptogyrin 1	*Syngr1*	2	3
49	GTTAGGAGCT	Syp synaptophysin	*Syp*	1	13
50	CCCCCAATTC	Vesicle-associated membrane protein 2	*Vamp2*	5	26

The table lists the genes that encode selected neuronal proteins of interest for neurotransmission. Data for the hippocampus SAGE library were taken from Datson *et al*. (2001). Tags below a count of two were not included in the list. Genes are listed in alphabetic order of the gene symbols. Transcript no represents arbitrary numbering of tags for easier citation in the text. Asterisks denote tags which are significantly more highly represented in either of the two libraries as calculated by the *z*-test (Ruijter *et al*., 2002): $*P < 0.05$; $**P < 0.001$.

FIG. 2. RNA *in situ* hybridization of selected genes derived from different tag abundance classes. Coronal sections of the SOC (left) and the hippocampus (right) were hybridized with DIG-labelled cRNA probes. Tag counts are indicated to the right as counts per 100 000 tags. (A and B) *Snap25*. Strong expression was observed throughout the SOC (335 tags). In the hippocampus (98 tags), *Snap25* was highly expressed in the pyramidal layer and moderately in the granular cells of the DG. (C and D) *AldoC*. Strong expression was found throughout the SOC (148 tags). In the hippocampus (18 tags), moderate expression was found in the pyramidal layer and the DG, and weak expression in the molecular layer. (E and F) *GrinA*. Moderate expression was found throughout the SOC (68 tags). In the hippocampus (16 tags), weak expression was found in the pyramidal layer and the DG. (G and H) *Calb1*. In the SOC 26 tags, high expression was restricted to the MNTB. In the hippocampus (13 tags), weak expression is observed in the pyramidal layer and the granular layer of the DG. In summary, most genes are expressed throughout the SOC and in the hippocampal pyramidal layer and the granular layer of the DG. MNTB; medial nucleus of the trapezoid body; MSO, medial superior olive; LSO, lateral superior olive; CA1–3, cornus ammon 1–3; DG, dentate gyrus. Scale bars, 250 μm (A, C, E and G); 500 μm (B, D, F and H).

large-scale determination of the number and relative abundance of transcripts of both known and unknown genes. This is a major advantage compared to array-based expression studies, which can only register mRNAs for which a probe exists on the array. In our SOC SAGE library, more than one-third of all unique tags (3679 out of 10 473, i.e. 35.1%) had no match in the current GenBank databases.

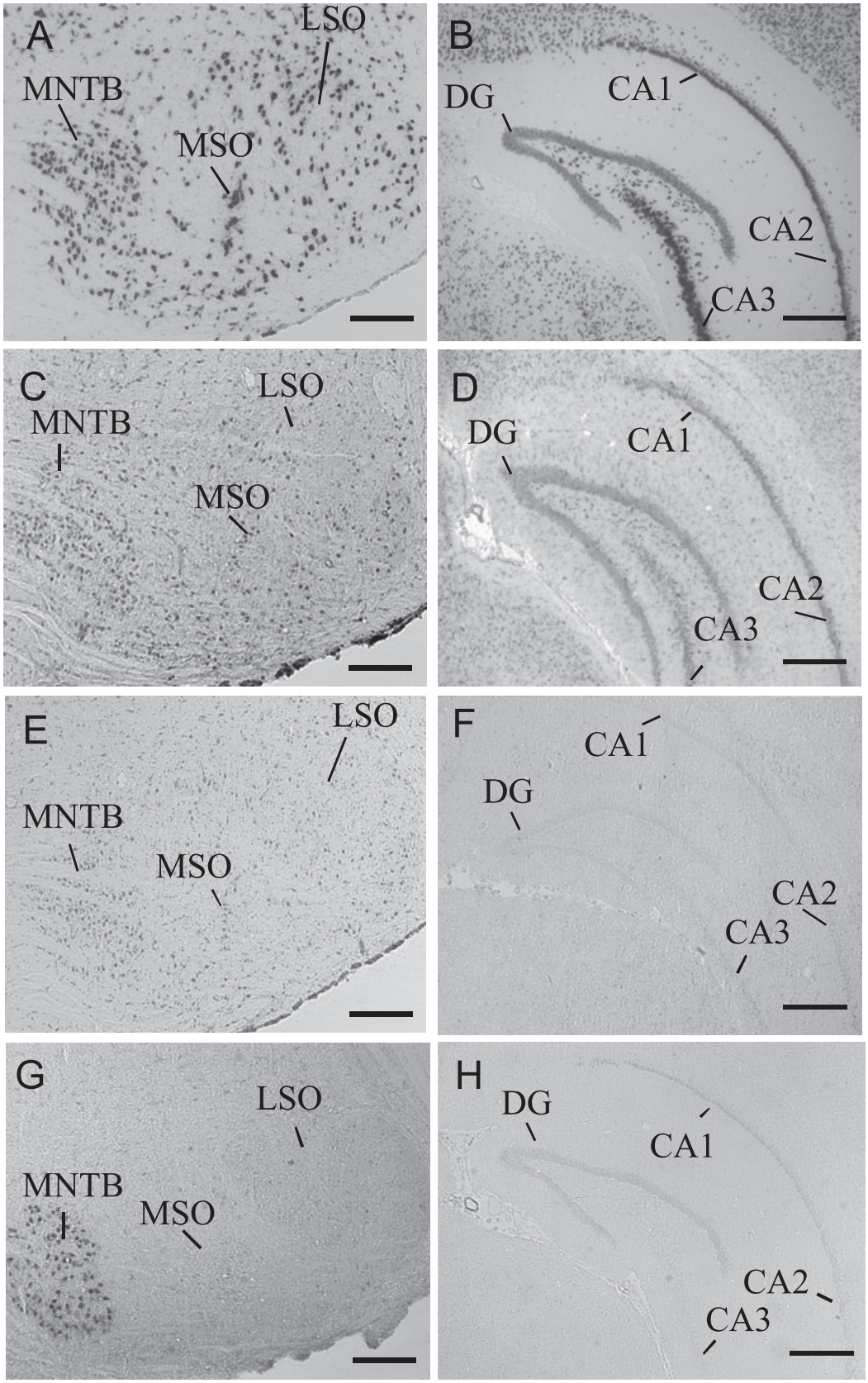

SAGE data obtained from the developing mouse neocortex revealed an even higher number, as 50% of the tags analysed remained unannotated (Gunnersen *et al*., 2002).

In theory, the entire transcriptome of a biological sample can be identified by SAGE. In practice, however, only medium- and high-abundant transcripts are identified due to the complexity of the transcriptome and the limited number of tags being sequenced (Gunnersen *et al*., 2002; Trendelenburg *et al*., 2002; Feldker *et al*., 2003). An expression analysis of various human tissues revealed that gene expression levels can range from 0.3 to 9417 transcript copies per cell and has identified more than 23 000 unique genes in the brain (Velculescu *et al*., 1999). Assuming a total of 300 000 transcripts per cell and a transcript that is expressed at one copy per cell, even the sequencing of approximately 1 200 000 tags will only result in a 97% probability of detecting at least one tag of this transcript (Velculescu *et al*., 1997; Trendelenburg *et al*., 2002). This is one reason why genes, for which no tag is detected by SAGE, can indeed be expressed in the tissue analysed. For example, the present study did not identify tags for the Kv1 channel subunits, the glycine transporter Glyt2, the purinergic receptor subunit P2rx4, the hyperpolarization-activated and cyclic-nucleotide-gated nonselective cation channels Hcn1–4, although they are present in the SOC (this study; Brew & Forsythe, 1995; Friauf *et al*., 1999; Grigg *et al*., 2000; Notomi & Shigemoto, 2004). A limitation of the expression analysis to medium- to high-abundant transcripts was also observed in hybridization-based experiments (Feldker *et al*., 2003) and appears to represent a general drawback in large-scale gene expression analyses. Another SAGE-specific limitation in gene identification is due to the fact that SAGE relies on the cleavage of cDNA molecules with a restriction enzyme to generate the tag. Transcripts with no appropriate restriction enzyme sequence (in our case a *Nla*III restriction site) therefore remain undetected; the proportion of such transcripts is estimated to be approximately 1% (Unneberg *et al*., 2003).

Validation of SAGE data by RNA in situ *hybridization*

To validate our SAGE data by an independent method, we used RNA *in situ* hybridization. We preferred this method to other techniques, such as real-time quantitative PCR or RNAse protection assays, because of the complex anatomical organization of the SOC. Only RNA *in situ* hybridization reveals the cellular distribution of identified transcripts. Furthermore, the same hippocampus tissue sample as used for the SAGE library by Datson *et al*. (2001) was unavailable for real-time PCR or Northernblot analysis. Most of the RNA probes gave signals throughout the SOC. The only exception was *Calb1*, which showed a strong expression exclusively in the MNTB. This complies well with a previous immunohistochemical analysis of calbindin in the SOC, in which the protein was mainly observed in the somata of MNTB neurons (Friauf, 1993).

The RNA *in situ* hybridization analysis confirmed furthermore the differences in tag counts between the SOC and the hippocampus, as in the latter, labelling was most often restricted to the pyramidal layer and the DG granular cells. The only exception was *Scn1b*, for which the RNA *in situ* data did not reflect the large difference in tag counts. Possible explanations are that the tag matches another, so far unknown transcript, or the occurrence of a splice variant in the hippocampus, which generates a different tag. For some of the genes, the labelling of individual cells also appeared stronger in the SOC than in the hippocampus.

Further validation of our SOC SAGE data comes from previous expression studies. *Ppia*, which is uniformly expressed in many tissues and therefore an internal control gene when comparing tissues (Feroze-Merzoug *et al*., 2002), had equal abundance in the two SAGE libraries (74 tags per 100 000 in the SOC and 75 tags per 100 000 in the hippocampus). Several tags, which were over-represented in the SOC library, encoded proteins that are more abundant in the SOC than in the hippocampus. These included MBP, PLP, Mobp (Foran & Peterson, 1992; Holz *et al*., 1996; Holz & Schwab, 1997), Kv3.1, Kv3.3 (Li *et al*., 2001; Weiser *et al*., 1994) and parvalbumin (Kawaguchi *et al*., 1987; Freund & Buzsaki, 1996; Lohmann & Friauf, 1996). In contrast, genes such as *Grin1*, *Gria2*, *Adora1*, *Htr5b*, *Nrgn* and *Calm1*, *Calm2* and *Calm3*, which encode proteins implicated in hippocampal long-term potentiation (Sanes & Lichtman, 1999), are indeed statistically more highly represented in the hippocampus than in the SOC.

The reliability of our SAGE data complies with previous analyses. Recent comparisons between SAGE and microarray expression data with Northern blot analysis or quantitative PCR revealed that SAGE data correlate more closely with the expression levels determined by an independent method than do those obtained through microarray analysis (Blackshaw *et al*., 2001; Anisimov *et al*., 2002). Nonetheless, it is important to recall that SAGE has several limitations that do not permit an absolute quantification of gene transcripts. As mentioned above, some transcripts do not possess the appropriate restriction enzyme cleavage site and therefore they are not detected by SAGE. Second, a given SAGE tag may match with different genes precluding any conclusion on the expression level of the matching genes without further analysis. Third, one gene can give rise to multiple tags due to polymorphisms and splice variants. Fourth, errors during reverse transcription, amplification of ditags, and during sequencing inevitably lead to wrong or nonexisting tags. Fifth, high-abundant tags may be underestimated because of duplicate ditag exclusion. Duplicate ditags are an intermediate product of the SAGE procedure and identical ones are only counted once, as in general, they are considered to represent amplification artifacts. However, highly abundant tags may form identical ditags before the amplification step and, thus, may not necessarily represent amplification products. Sixth, some transcripts, e.g. those encoding some nuclear proteins, are not polyadenylated. These transcripts will not be identified by SAGE because the mRNAs are captured initially via their poly(A)$^+$ tail.

FIG. 3. Expression analysis of the purinergic receptors subunits $P2X_6$ and $P2X_4$. (A and B) RNA *in situ* hybridization of *P2rx6* in coronal sections of the SOC (A) and hippocampus (B). Strong expression was observed throughout the SOC and in the hippocampal pyramidal layer and the DG. (C and D) Immunoreactivity to the $P2X_6$ subunit antibody in a coronal section through the SOC (C) and a sagittal section through the hippocampus (D) of rats aged P60. In the SOC, strong immunoreactivity is observed in the LSO and the MNTB. In the hippocampus; immunoreactivity is predominant in the CA1 to CA2 and, to a lesser extent, in the CA3 region, the hilus, and the DG. (E–G) High magnification photomicrograph of the MNTB (E and F) and the LSO (G). In MNTB neurons, $P2X_6$ immunoreactivity is localized in neuronal somata and primary dendrites (E). Preadsorption of purified $P2X_6$ antibody with the corresponding fusion protein resulted in no signal (F), demonstrating the specificity of the P2rx6 staining. In LSO neurons, labelling is observed in most neurons and extends from cell bodies to proximal dendrites (G). (H and I) RNA *in situ* hybridization of antisense *P2X4* cRNA to coronal sections of the SOC (H) and the hippocampus (I). Strong expression was observed throughout the SOC and in the hippocampal pyramidal layer and the DG. Abbreviations as in legend to Fig. 2. Scale bar, 250 μm (A and H); 500 μm (B and I); 200 μm (C); 400 μm (D); 20 μm (E–G).

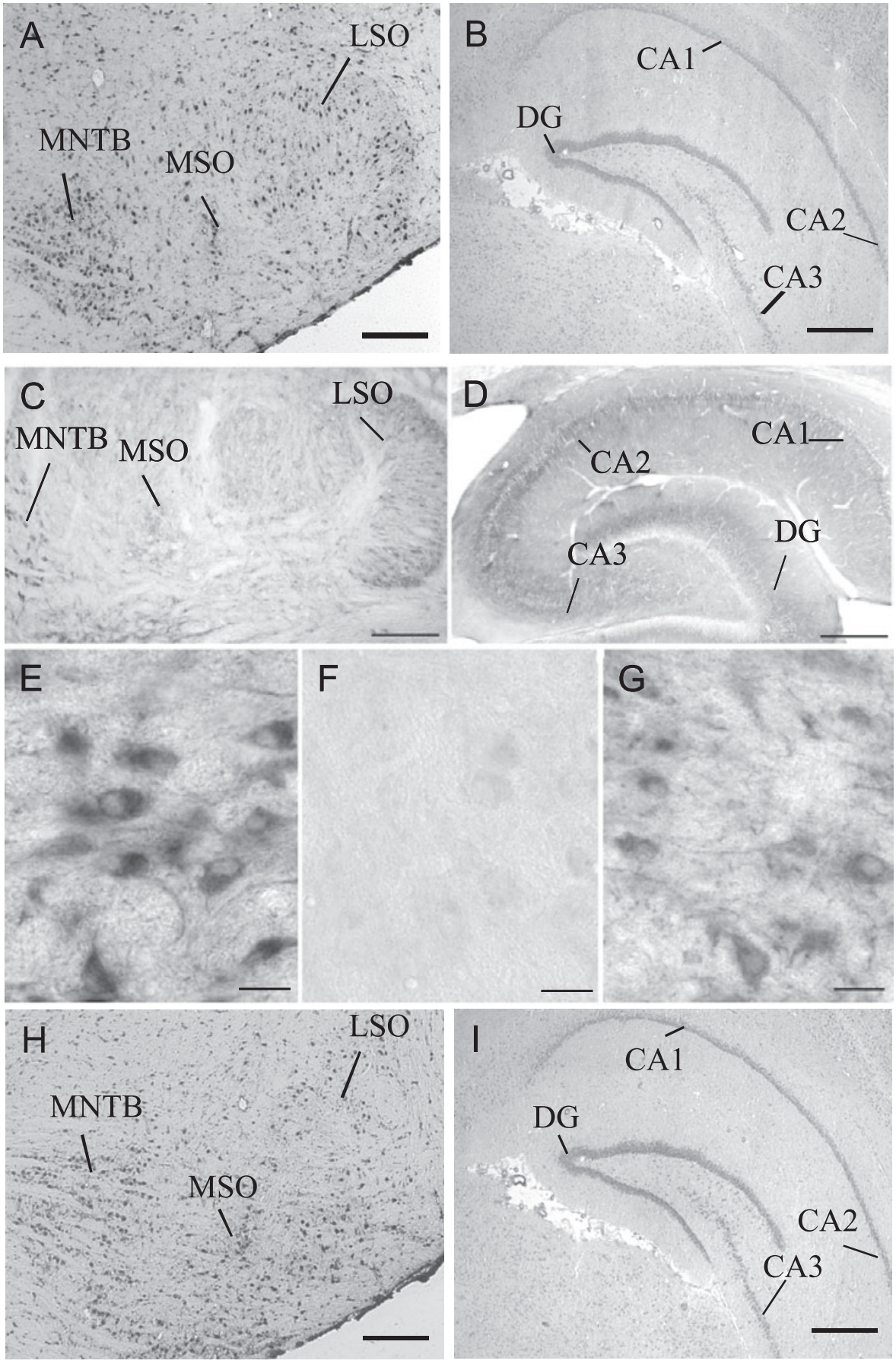
A
LSO
MNTB
MSO
B
CA1
DG
CA2
CA3
C
LSO
MNTB
MSO
D
CA1
CA2
CA3
DG
E
F
G
H
LSO
MNTB
MSO
I
CA1
DG
CA2
CA3

Finally, low-abundant tags show considerable quantitative variations as SAGE is a sampling method with a finite number of sequenced tags. Therefore, low-abundant tags have a low probability of being detected (Anisimov *et al*., 2002; Stern *et al*., 2003). Due to this fact, we excluded tags with counts less than five from our comparative analysis between the SOC and the hippocampus.

Abundant transcripts in the SOC compared to hippocampus

We compared the gene expression pattern between the SOC and hippocampus to identify genes important for SOC neurons. Whereas the SOC is part of the pontine auditory brainstem and involved in fundamental aspects of information processing within a sensory pathway (sound localization), the hippocampus is a telencephalic structure mainly involved in cognitive aspects (learning and memory formation). The difference in function is reflected by a difference in gene expression. More than 30% of the tags with counts greater than four were differentially expressed between these two brain regions at a *P*-value < 0.05, and more than 4% at a *P*-value $< 10^{-5}$. Applying the same criteria to four SAGE libraries from mouse lateral and medial striatum, nucleus accumbens, and somatosensory cortex (de Chaldée *et al*., 2003), the greatest differences in tag abundance were 26.1% at a *P*-value < 0.05 (medial striatum against somatosensory cortex) and 1.4% at a *P*-value $< 10^{-5}$ (medial striatum against somatosensory cortex) The higher number of differentially expressed genes between the SOC and the hippocampus may indicate larger functional differences compared to the differences between the four above-mentioned mouse brain regions. Another explanation might be that the SOC and the hippocampus have very distinct developmental origins. This explanation gains support by a comparative microarray-based expression analysis of hippocampus, entorhinal cortex, midbrain, and cerebellum. The cerebellum was the most distinct region, followed by the midbrain, and this order is in line with the differences in developmental origin (Pavlidis & Nobel, 2001). Nevertheless, to address this issue, further expression analyses have to be performed, for example, in the auditory midbrain or the auditory cortex.

Several genes were found to be statistically more abundant in the SOC than in the hippocampus. These include genes involved in energy metabolism, such as glucose transport, the glycolytic pathway and the tricarbon acid cycle, ATP synthesis and the energy transfer between mitochondria and the cytosol. The abundance of these transcripts in the SOC complies with previous data on the energy consumption in the brain (Sokoloff, 1981). Radioactive deoxyglucose measurements demonstrated the highest values of glucose utilization in structures involved in auditory functions. The glucose utilization of the SOC was 133 ± 7 μmoles/100 g per minute and thus approximately twice as high as in the hippocampus (79 ± 3 μmoles/100 g per minute) (Sokoloff, 1981). The high energy consumption in the auditory system is likely due to the high average firing rate of the neurons in this sensory pathway, as demonstrated by a recent thorough theoretical calculation of the energy expenditure of excitatory signalling in rodents (Attwell & Laughlin, 2001). An additional explanation for the high expression level of some genes involved in energy metabolism may be the fact that the tricarbon acid cycle is closely coupled to the generation of the neurotransmitters glutamate and glycine (Mackenzie & Erickson, 2004). These two molecules are the main neurotransmitters in the SOC (Friauf *et al*., 1997) and are likely required in large amounts to ensure high frequency firing rates.

Another highly expressed gene class encodes proteins important for myelination. Among them is the channel protein Kir4.1, which was recently shown to play an important role in *in vivo* myelination (Neusch *et al*., 2001). Oligodendrocytes of Kir4.1 knockout mice lack most of the wild-type K^+-conductance, have depolarized membrane potentials, and display hypomyelination.

Our SAGE analysis detected several interesting candidates involved in fast and reliable synaptic transmission. Mainly, genes involved in neurotransmitter synthesis, storage, and release were found to be abundant in the SOC. Four of the encoded proteins (Glud1, Glns, Snat2, Snat3) are involved in the so-called glutamate–glutamine cycle in the brain, which is important to replenish neurons with glutamine (Mackenzie & Erickson, 2004). Glutamine serves as an energy substrate for oxidative phosphorylation in the tricarbon acid cycle. Alternatively, it can be used to generate the neurotransmitters glutamate, GABA, and glycine. The conversion of glutamate to GABA requires the enzyme glutamate decarboxylase (Gad), and the synthesis of glycine requires the serine hydroxymethyl transferase (Shmt). For Gad, only one tag was detected, whereas for Shmt, 32 tags were observed in the library. This finding complies well with the fact that glycine represents the major inhibitory neurotransmitter in the adult SOC (Friauf *et al*., 1997). To release neurotransmitters, a recent study in chromaffin cells pointed to an important role of *SNAP25* (104 tags), another gene that is significantly more highly represented in the SOC than in the hippocampus. In the absence of this protein, vesicle docking persisted, but primed vesicle pools were empty and fast calcium-triggered release abolished (Sorensen *et al*., 2003).

Concerning neurotransmitter receptors, only a few genes were identified by SAGE. Among them was the gene encoding the purinergic receptor subunit $P2X_6$. Expression analysis at both the RNA and the protein level confirmed its presence in the SOC. All major nuclei (MNTB, LSO, MSO) express $P2X_6$ subunits. As $P2X_6$ subunits alone do not appear to form functional channels when expressed in heterologous expression systems (Khakh, 2001), we also analysed the expression of *P2rx4*, as the encoded protein $P2X_4$ can form heteromeric receptors with $P2X_6$ subunits. The overlapping expression pattern found for the *P2rx4* and *P2rx6* genes suggests functional purinergic receptors in the SOC. The function of P2X receptors in the SOC is obscure and will depend much on their localization, i.e. whether they are pre- or postsynaptic. Our immunocytochemical data indicate at least a postsynaptic location in SOC neurons, but this needs to be analysed more rigorously by electron microscopy. In addition, electrophysiological analysis should be performed to dissect the function of P2X receptors in the auditory brainstem.

Taken together, our SAGE analysis identified several promising candidate genes for the specific properties of auditory neurons, for example high-frequency and high-secure neurotransmission. This list, however, is not complete, as several important gene classes with low transcription rates, such as those for membrane proteins, are under-represented in global gene expression analyses. Furthermore, the SOC is composed of several nuclei and our SAGE data represent the analysis of the entire SOC. Thus, genes being important for only one of the nuclei such as MNTB or LSO, have possibly in part escaped detection, and a refined analysis of individual nuclei will be required. In addition, gene expression levels are not strictly linked to the functional role of the encoded proteins, and detailed characterization of the identified candidate genes will be required to prove their predicted important role. Functional analyses of several genes identified by our approach have, however, already demonstrated their importance for the tissue in which they are over-represented. Deletion of *Kcnc1*, which is significantly over-represented in the SOC, results in failure of MNTB neurons to follow high-frequency stimulation (Macica *et al*., 2003) and *Grin1*, being significantly over-represented in the hippocampus, was shown to be important for long-term potentiation in the hippocampus (Nicoll & Malenka, 1999).

In summary, we have generated the first large-scale transcriptome analysis of an auditory processing centre. Although it is not fully comprehensive, the SAGE catalogue represents an approximate 50-fold increase in our knowledge of genes expressed in the SOC. It thus provides an important tool towards the characterization of the molecular machinery underlying auditory information processing. Furthermore, it serves as a reference for further expression studies. Gene expression is highly dynamic and a function of development, differentiation, ageing, and disease. Thus, a SAGE analysis of the immature SOC and its comparison with the SAGE data presented here is likely to provide further insight into transcriptome changes underlying maturation. This analysis, together with other ongoing large-scale gene expression analyses in the auditory system will also be instrumental in the identification of stage- and centre-specific promoters (Friedland *et al*., 2004; A. Koehl & H.G. Nothwang, unpublished). These promoters can be used to generate highly region-specific transgenic animals in order to determine the function of the identified genes in the SOC *in vivo* and *in vitro*.

Supplementary material

The following supplementary material may be found on:

http://www.blackwellpublishing.com/products/journals/suppmat/EJN3791/EJN3791sm.htm

Fig. S1. RNA *in situ* hybridization of selected genes derived from different tag abundance classes.

Table S1. Oligonucleotides used for gene-specific expression analysis.

Table S2. Comparative quantitative analysis between SOC and hippocampus of 11 major transcripts involved in the formation and function of myelin sheaths.

Table S3. Comparison between transcriptome and proteome analysis in the SOC.

Acknowledgements

We wish to thank S. Sauer for help with the SAGE protocol, M. Nuhn, J. Ruijter and M.Z. Man for help with the statistical analysis, and K. Ociepka for help with the RNA *in situ* hybridization. Funding for this research project was provided by a grant from the Deutsche Forschungsgemeinschaft to H.G.N and E.F (No428/1–1) and to F.S. (So390/1–1), and by the Nano+Bio-Center Kaiserslautern.

Abbreviations

DG, dentate gyrus; DIG, digoxigenin; EST, expressed sequence tag; LSO, lateral superior olive; MNTB, medial nucleus of the trapezoid body; MSO, medial superior olive; P, postnatal day; SAGE, serial analysis of gene expression; SOC, superior olivary complex.

References

Anisimov, S.V., Tarasov, K.V., Stern, M.D., Lakatta, E.G. & Boheler, K.R. (2002) A quantitative and validated SAGE transcriptome reference for adult mouse heart. *Genomics*, **80**, 213–222.

Attwell, D. & Laughlin, S.B. (2001) An energy budget for signaling in the grey matter of the brain. *J. Cereb. Blood Flow Metabol.*, **21**, 1133–1145.

Becker, M., Nothwang, H.G. & Friauf, E. (2003) Differential expression pattern of chloride cotransporters *NCC, NKCC2, KCC1, KCC3, KCC4* and *AE3* in the developing rat auditory brainstem. *Cell Tissue Res.*, **312**, 155–165.

Blackshaw, S., Fraioli, R.E., Furukawa, T. & Cepko, C.L. (2001) Comprehensive analysis of photoreceptor gene expression and the identification of candidate retinal disease genes. *Cell*, **107**, 579–589.

Brew, H.M. & Forsythe, I.D. (1995) Two voltage-dependent K^+ conductances with complementary functions in postsynaptic integration at a central auditory synapse. *J. Neurosci.*, **15**, 8011–8022.

de Chaldée, M., Gaillard, M.C., Bizat, N., Buhler, J.M., Manzoni, O., Bockaert, J., Hantraye, P., Brouillet, E. & Elalouf, J.M. (2003) Quantitative assessment of transcriptome differences between brain territories. *Genome Res.*, **13**, 1646–1653.

Cheval, L., Virlon, B. & Elalouf, J.M. (2000) SADE: a microassay for serial analysis of gene expression. In Hunt, S.P. & Livesey, F.J., (Eds), *Functional Genomics*. Oxford University Press, Oxford, pp. 139–163.

Collo, G., North, R.A., Kawashima, E., Merlo-Pich, E., Neidhart, S., Surprenant, A. & Buell, G. (1996) Cloning of P2X5 and P2X6 receptors and the distribution and properties of an extended family of ATP-gated ion channels. *J. Neurosci.*, **16**, 2495–2507.

Datson, N.A., van der Perk, J., de Kloet, E.R. & Vreugdenhil, E. (2001) Expression profile of 30 000 genes in rat hippocampus using SAGE. *Hippocampus*, **11**, 430–444.

Feldker, D.E.M., Datson, N.A., Veenema, A.H., Meulmeester, E., de Kloet, E.R. & Vreugdenhil, E. (2003) Serial analysis of gene expression predicts structural differences in hippocampus of long attack latency and short attack latency mice. *Eur. J. Neurosci.*, **17**, 379–387.

Feroze-Merzoug, F., Berquin, I.M., Dey, J. & Chen, Y.Q. (2002) Peptidylprolyl isomerase A (PPIA) as a preferred internal control over GAPDH and beta-actin in quantitative RNA analyses. *Biotechniques*, **32**, 776–778.

Foran, D.R. & Peterson, A.C. (1992) Myelin acquisition in the central nervous system of the mouse revealed by an MBP-Lac Z transgene. *J. Neurosci.*, **12**, 4890–4897.

Freund, T.F. & Buzsaki, G. (1996) Interneurons in the hippocampus. *Hippocampus*, **6**, 347–470.

Friauf, E. (1993) Transient appearance of calbindin-D_{28k}-positive neurons in the superior olivary complex of developing rats. *J. Comp. Neurol.*, **334**, 59–74.

Friauf, E., Aragón, C., Löhrke, S., Westenfelder, B. & Zafra, F. (1999) Developmental expression of the glycine transporter GLYT2 in the auditory system of rats suggests involvement in synapse maturation. *J. Comp. Neurol.*, **412**, 17–37.

Friauf, E., Kandler, K., Lohmann, C. & Kungel, M. (1997) Inhibitory and excitatory brainstem connections involved in sound localization: how do they develop? In Syka, J., (Ed), *Acoustical Signal Processing in the Central Auditory System*. Plenum, New York, pp. 181–191.

Friedland, D.R., Raphael, R., Hansen, A.R., Popper, P. & Cioffi, J.A. (2004) Gene expression in the anterior ventral cochlear nucleus. *Proc. Assoc. Res. Otolaryngol.*, **27**, 307.

von Gersdorff, H. & Borst, J.G.G. (2002) Short-term plasticity at the calyx of Held. *Nature Rev. Neurosci.*, **3**, 53–64.

Gibbs, R.A., Weinstock, G.M., Metzker, M.L., Muzny, D.M., Sodergren, E.J., Scherer, S., Scott, G., Steffen, D., Worley, K.C., Burch, P.E. (2004) Genome sequence of the Brown Norway rat yields insights into mammalian evolution. *Nature*, **428**, 493–521.

Grigg, J.J., Brew, H.M. & Tempel, B.L. (2000) Differential expression of voltage-gated potassium channel genes in auditory nuclei of the mouse brainstem. *Hearing Res.*, **140**, 77–90.

Grothe, B. (2003) New roles for synaptic inhibition in sound localization. *Nature Rev. Neurosci.*, **4**, 1–11.

Gunnersen, J.M., Augustine, C., Spirkoska, V., Kim, M., Brown, M. & Tan, S.S. (2002) Global analysis of gene expression patterns in developing mouse neocortex using serial analysis of gene expression. *Mol. Cell. Neurosci.*, **19**, 560–573.

Holz, A., Schaeren-Wiemers, N., Schaefer, C., Pott, U., Colello, R.J. & Schwab, M.E. (1996) Molecular and developmental characterization of novel cDNAs of the myelin-associated/oligodendrocytic basic protein. *J. Neurosci.*, **16**, 467–477.

Holz, A. & Schwab, M.E. (1997) Developmental expression of the myelin gene MOBP in the rat nervous system. *J. Neurocytol.*, **26**, 467–477.

Jasper, H., Benes, V., Schwager, C., Sauer, S., Clauder-Munster, S., Ansorge, W. & Bohmann, D. (2001) The genomic response of the *Drosophila* embryo to JNK signaling. *Dev. Cell*, **1**, 579–586.

Kawaguchi, Y., Katsumaru, H., Kosaka, T., Heizmann, C.W. & Hama, K. (1987) Fast spiking cells in the rat hippocampus (CA1 region) contain the calcium-binding protein parvalbumin. *Brain Res.*, **416**, 369–374.

Khakh, B.S. (2001) Molecular physiology of P2X receptors and ATP signalling at synapses. *Nature Rev. Neurosci.*, **2**, 165–174.

Kim, G. & Kandler, K. (2003) Elimination and strengthening of glycinergic/GABAergic connections during tonotopic map formation. *Nature Neurosci.*, **6**, 282–290.

Koehl, A., Friauf, E. & Nothwang, H.G. (2003) Efficient cloning of SAGE tags by blunt-end ligation of polished concatemers. *Biotechniques*, **34**, 692–694.
Lander, E.S., Linton, L.M., Birren, B., Nusbaum, C., Zody, M.C., Baldwin, J., Devon, K., Dewar, K., Doyle, M. & FitzHugh, W. (2001) Initial sequencing and analysis of the human genome. *Nature*, **409**, 860–921.
Li, W., Kaczmarek, L.K. & Perney, T.M. (2001) Localization of two high-threshold potassium channel subunits in the rat central auditory system. *J. Comp. Neurol.*, **437**, 196–218.
Lohmann, C. & Friauf, E. (1996) Distribution of the calcium-binding proteins parvalbumin and calretinin in the auditory brainstem of adult and developing rats. *J. Comp. Neurol.*, **367**, 90–109.
Macica, C.M., von Hehn, C.A.A., Wang, L.Y., Ho, C.S., Yokoyama, S., Joho, R.H. & Kaczmarek, L.K. (2003) Modulation of the Kv3.1b potassium channel isoform adjusts the fidelity of the firing pattern of auditory neurons. *J. Neurosci.*, **23**, 1133–1141.
Mackenzie, B. & Erickson, J.D. (2004) Sodium-coupled neutral amino acid (System N/A) transporters of the SLC38 gene family. *Pflugers Arch.*, **447**, 784–795.
Nabekura, J., Katsurabayashi, S., Kakazu, Y., Shibata, S., Matsubara, A., Jinno, S., Mizoguchi, Y., Sasaki, A. & Ishibashi, H. (2004) Developmental switch from GABA to glycine release in single central synaptic terminals. *Nature Neurosci.*, **7**, 17–23.
Neusch, C., Rozengurt, N., Jacobs, R.E., Lester, H.A. & Kofuji, P. (2001) Kir4.1 potassium channel subunit is crucial for oligodendrocyte development and *in vivo* myelination. *J. Neurosci.*, **21**, 5429–5438.
Nicoll, R.A. & Malenka, R.C. (1999) Expression mechanisms underlying NMDA receptor-dependent long-term potentiation. *Ann. NY Acad. Sci.*, **868**, 15–25.
North, R.A. (2002) Molecular physiology of P2X receptors. *Physiol. Rev.*, **82**, 1013–1067.
Nothwang, H.G., Becker, M., Ociepka, K. & Friauf, E. (2003) Protein analysis in the rat auditory brainstem by two-dimensional gel electrophoresis and mass spectrometry. *Mol. Brain Res.*, **116**, 59–69.
Notomi, T. & Shigemoto, R. (2004) Immunohistochemical localization of I-h channel subunits, HCN1–4, in the rat brain. *J. Comp. Neurol.*, **471**, 241–276.
Oertel, D. (1999) The role of timing in the brain stem auditory nuclei of vertebrates. *Annu. Rev. Physiol.*, **61**, 497–519.
Pavlidis, P. & Nobel, W.S. (2001) Analysis of strain and regional variation in gene expression in mouse brain. *Genome Biol.*, **2**, 42.1–42.42.15.
Ruan, Y.J., Le Ber, P., Ng, H.H. & Liu, E.T. (2004) Interrogating the transcriptome. *Trends Biotechnol.*, **22**, 23–30.
Rubio, M.E. & Soto, F. (2001) Distinct localization of P2X receptors at excitatory postsynaptic specializations. *J. Neurosci.*, **21**, 641–653.
Ruijter, J.M., van Kampen, A.H.C. & Baas, F. (2002) Statistical evaluation of SAGE libraries: consequences for experimental design. *Physiol. Genomics*, **11**, 37–44.
Sanes, D.H. & Friauf, E. (2000) Development and influence of inhibition in the lateral superior olivary nucleus. *Hearing Res.*, **147**, 46–58.
Sanes, J.R. & Lichtman, J.W. (1999) Can molecules explain long-term potentiation? *Nature Neurosci.*, **2**, 597–604.
Schneggenburger, R., Sakaba, T. & Neher, E. (2002) Vesicle pools and short-term synaptic depression: lessons from a large synapse. *TINS*, **25**, 206–212.
Sokoloff, L. (1981) Localisation of functional activity in the central nervous system by measurement of glucose utilization with radioactive deoxyglucose. *J. Cereb. Blood Flow Metabol.*, **1**, 7–36.
Sorensen, J.B., Nagy, G., Varoqueaux, F., Nehring, R.B., Brose, N., Wilson, M.C. & Neher, E. (2003) Differential control of the releasable vesicle pools by SNAP-25 splice variants and SNAP-23. *Cell*, **114**, 75–86.
Stern, M.D., Anisimov, S.V. & Boheler, K.R. (2003) Can transcriptome size be estimated from SAGE catalogs? *Bioinformatics*, **19**, 443–448.
Trendelenburg, G., Prass, K., Priller, J., Kapinya, K., Polley, A., Muselmann, C., Ruscher, K., Kannbley, U., Schmitt, A.O., & Castell, S. (2002) Serial analysis of gene expression identifies metallothionein-II as major neuroprotective gene in mouse focal cerebral ischemia. *J. Neurosci.*, **22**, 5879–5888.
Trussell, L.O. (1999) Synaptic mechanisms for coding timing in auditory neurons. *Annu. Rev. Physiol.*, **61**, 477–496.
Unneberg, P., Wennborg, A. & Larsson, M. (2003) Transcript identification by analysis of short sequence tags-influence of tag length, restriction site and transcript database. *Nucl. Acids Res.*, **31**, 2217–2226.
Velculescu, V.E., Zhang, L. & Lash, A.E., Yu, J., Rago, C., Lal, A., Wang, C.J., Beaudry, G.A., Ciriello, K.M. & Cook, B.P. (1999) Analysis of human transcriptomes. *Nature Genet.*, **23**, 387–388.
Velculescu, V.E., Zhang, L., Vogelstein, B. & Kinzler, K.W. (1995) Serial analysis of gene expression. *Science*, **270**, 484–487.
Velculescu, V.E., Zhang, L., Zhou, W., Vogelstein, J., Basrai, M.A., Bassett, D.E., Hieter, P., Vogelstein, B. & Kinzler, K.W. (1997) Characterization of the yeast transcriptome. *Cell*, **88**, 243–251.
Waterston, R.H., Lindblad-Toh, K., Birney, E., Rogers, J., Abril, J.F., Agarwal, P., Agarwala, R., Ainscough, R., Alexandersson, M., & An, P. (2002) Initial sequencing and comparative analysis of the mouse genome. *Nature*, **420**, 520–562.
Weiser, M., Vega-Saenz, D. M., Kentros, C., Moreno, H., Franzen, L., Hillman, D., Baker, H. & Rudy, B. (1994) Differential expression of Shaw-related K^+ channels in the rat central nervous system. *J. Neurosci.*, **14**, 949–972.